

# Water Lone Pair Delocalization in Classical and Quantum Descriptions of the Hydration of Model Ions

Richard C. Remsing,<sup>\*,†</sup> Timothy T. Duignan,<sup>‡</sup> Marcel D. Baer,<sup>‡</sup> Gregory K. Schenter,<sup>‡</sup> Christopher J. Mundy,<sup>\*,‡,||</sup> and John D. Weeks<sup>\*,§</sup>

<sup>†</sup>Institute for Computational Molecular Science, Temple University, Philadelphia, Pennsylvania 19122, United States

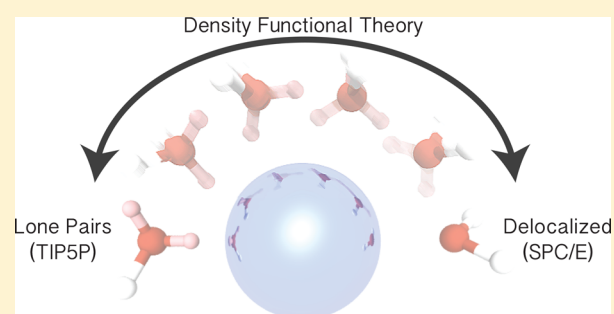
<sup>‡</sup>Chemical and Materials Science Division, Pacific Northwest National Laboratory, Richland, Washington, United States

<sup>§</sup>Institute for Physical Science and Technology and Department of Chemistry and Biochemistry, University of Maryland, College Park, Maryland 20742, United States

<sup>||</sup>Affiliate Professor, Department of Chemical Engineering, University of Washington, Seattle, Washington, United States

## S Supporting Information

**ABSTRACT:** Understanding the nature of ionic hydration at a fundamental level has eluded scientists despite intense interest for nearly a century. In particular, the microscopic origins of the asymmetry of ion solvation thermodynamics with respect to the sign of the ionic charge remains a mystery. Here, we determine the response of accurate quantum mechanical water models to strong nanoscale solvation forces arising from excluded volumes and ionic electrostatic fields. This is compared to the predictions of two important limiting classes of classical models of water with fixed point charges, differing in their treatment of “lone pair” electrons. Using the quantum water model as our standard of accuracy, we find that a single fixed classical treatment of lone pair electrons cannot accurately describe solvation of both apolar and cationic solutes, emphasizing the need for a more flexible description of local electronic effects in solvation processes. However, we explicitly show that all water models studied respond to weak long-ranged electrostatic perturbations in a manner that follows macroscopic dielectric continuum models, as would be expected. We emphasize the importance of these findings in the context of realistic ion models, using density functional theory and empirical models, and discuss the implications of our results for quantitatively accurate reduced descriptions of solvation in dielectric media.



## INTRODUCTION

Ion hydration is a far-reaching and fundamental process in nature, acting as a fundamental driving force for processes like salting out of biomolecules from solution,<sup>1,2</sup> stabilization or unfolding of proteins by the addition of protectants or denaturants,<sup>2–4</sup> respectively, and many important processes in atmospheric chemistry.<sup>5–9</sup> Despite its importance, the solvation of ions in water is not completely understood. Nearly a century ago, Max Born introduced a dielectric continuum theory (DCT) model for ion solvation where the uniform solvent (water) was treated as a dielectric continuum that responded linearly and locally to an imposed charge distribution.<sup>10</sup> The simple Born model for ion solvation considered the hydration free energy of an ion to be equivalent to that generated by a point charge at the center of a cavity located inside an otherwise uniform dielectric medium.

Despite its simplicity, this DCT approach reproduced the order of magnitude of experimentally determined ion hydration free energies but was unable to capture significant qualitative features of ion hydration. Specifically, for ions of the same size, anions are more favorably hydrated than cations, an important

phenomenon that naive linear DCT models are unable to describe.

Previous attempts to explain the asymmetry of ion hydration, even from atomistic principles, have relied on ascribing different effective sizes to cationic and anionic solutes, even when modeled with the same neutral excluded volume cores.<sup>11–14</sup> This allowed for the development of empirical extensions of the Born model that can be fit to experimental data with quantitative accuracy. The explanation of thermodynamics in terms of the ion size seems to indicate that the solute is the source of hydration asymmetries, but the use of effective radii implicitly accounts for solvent effects, like a spatially varying dielectric constant, as illustrated in the [Supporting Information](#). Recent work has further highlighted that much of the asymmetry of solvation thermodynamics with respect to ion

**Special Issue:** Benjamin Widom Festschrift

**Received:** October 30, 2017

**Revised:** December 24, 2017

**Published:** January 29, 2018

charge must originate from the response of the solvent network to strong local perturbations.<sup>15–23</sup>

This revelation immediately leads to questions regarding the molecular sophistication of water models that are needed to obtain physically accurate ion hydration free energies. Treating the solvent as a uniform dielectric medium is too simplistic a description in many cases, and most state-of-the-art studies rely on empirical point charge models of water to provide a more detailed description of ionic hydration. This asymmetric response of the solvent is unlikely to be the only contribution to the difference in the solvation free energy of real cations and anions of the same size. Differences in the direct dispersion, exchange, and induction interactions of the ions with the solvent molecules will also play a role, although these terms will partially compensate each other.<sup>24–27</sup>

Deeper insights into the description of water necessary for describing ion hydration can be made by monitoring perturbations of the solvent that are induced by nanoscale broken symmetries across a range of water models, including those described from first-principles. Such broken symmetries in the context of this paper arise from a hard spherical solute, an electrostatic field arising from an embedded ionic charge distribution, or a combination of the two. This allows us to systematically probe the origins of the asymmetric solvent response that underlie the charge asymmetry of ion hydration. We have previously shown that this approach can uncover surprising differences between empirical model descriptions of the solute size dependence of uncharged hard sphere solvation.<sup>22</sup>

In this work, we compare the predictions of fundamentally different water models to the nanoscale electrostatic and excluded volume perturbations that generate the asymmetries observed in ion hydration thermodynamics. The models lie at opposite extremes of a spectrum of water model complexity and flexibility, where flexibility here refers to the ability of the molecular charge distribution to respond to its environment. The simplest models are classical, empirical models with fixed charge distributions reflecting different limiting descriptions of “lone pair” electrons.<sup>22,28</sup> These simple fixed descriptions are contrasted with the inherently more flexible quantum density functional treatments of the electron density of water.

We find that classical, fixed-charge, empirical potentials cannot simultaneously describe the response of water to apolar and ionic solutes, suggesting that significant changes to the current approach of using fixed charge empirical water models are needed. The observed model dependencies are demonstrated to arise from different responses to strong local perturbations. In contrast, long-ranged properties, like the dielectric constant, are essentially model independent and predicted accurately by both the fixed-charge classical- and quantum-mechanical models. Indeed, we show that both classical- and quantum-mechanical descriptions of water quantitatively agree in their long-ranged dielectric response to (spatially) slowly varying electrostatic fields, which in turn follows expectations from DCT.<sup>23</sup> This important finding justifies much of our current understanding of screening in aqueous solutions, which relies on treating water as a dielectric medium. Finally, we adapt our findings to describe the hydration of physical ion models, as described by empirical potentials or with *ab initio* methods, before placing our results in a broader context and discussing implications for developing accurate models of ionic hydration.

## METHODS

**Simulation of Point Charge Models.** Classical molecular dynamics (MD) simulations of the empirical three-site extended simple point charge (SPC/E)<sup>29</sup> and five-site transferable intermolecular potential (TIP5P)<sup>30</sup> models of water were performed using DL\_POLY version 2.18,<sup>31</sup> suitably modified to include the potentials used throughout this work. The hard sphere excluded volume with radius  $R$  interacts with a water oxygen nucleus at a distance  $r > R$  from the cavity center through the potential used previously:<sup>22</sup>

$$V(r) = 1 - \tanh\left(\frac{r - R}{0.02 \text{ \AA}}\right) \quad (1)$$

All simulations were performed in the isothermal–isobaric (NPT) ensemble to maintain the system at an average density. A temperature and pressure of 300 K and 1 atm were maintained using a Berendsen thermostat and barostat, respectively.<sup>32</sup> The evaluation of electrostatic interactions employed the Ewald summation method,<sup>33</sup> and neutrality was maintained through the addition of a neutralizing uniform background charge density whenever the solute was charged. Charging free energies of the hard spheres,  $\Delta G_Q$ , were computed following previous work<sup>34</sup> by using eq 4 (discussed below) and numerically evaluating the integral with the coupling parameter  $\lambda$  incremented by  $\Delta\lambda = 0.1$ . Sodium and chloride ions were modeled using the parameters developed by Horinek et al.<sup>35</sup>

**Density Functional Theory Molecular Dynamics Simulations.** All DFT-based simulations employed the CP2K software package.<sup>36</sup> Energies and forces were evaluated for MD within the QUICKSTEP module,<sup>36</sup> which contains an accurate and efficient implementation of DFT employing dual basis sets of Gaussian-type orbitals (molopt-DZV2P) and plane waves (expanded to 400 Ry) for the electron density.<sup>37</sup> Simulations for the charging of a 2.6 Å sphere utilized the same system size geometry and protocol as described in ref 34. Total trajectory lengths of 25 ps were utilized for charged hard sphere cavities, and 50 ps was used for the neutral hard sphere cavities. For the larger 4 Å charged cavities, a slab geometry was utilized, as was discussed in detail in ref 22. A trajectory of 50 ps was needed for satisfactory convergence of the positively charged hard sphere, and 30 ps was used for the negatively charged hard sphere. We only explicitly considered the valence electrons, with core electrons represented by Goedecker–Teter–Hutter pseudopotentials.<sup>38</sup> We used the revised Perdew, Burke, and Ernzerhof (revPBE) functional<sup>39,40</sup> with the D3 dispersion correction, introduced by Grimme.<sup>41–43</sup> The standard three-dimensional Ewald convention was used, with neutrality maintained via a neutralizing background.<sup>33</sup> A constant temperature of 300 K was maintained using a Nosé–Hoover chain thermostat of length 3 coupled to each molecule, and the equations of motion were integrated with a time step of 0.5 fs.

## EMPIRICAL FIXED CHARGE WATER MODELS CANNOT SIMULTANEOUSLY DESCRIBE IONIC AND APOLAR HYDRATION

Hydration structure is intimately tied to the thermodynamics of solvation. Thus, to understand the molecular underpinnings of ion hydration thermodynamics, we focus on the structural response of the different representations of liquid water to the simplest model ion, namely, a charged hard sphere. This crude description of an ion allows us to compare the hydration

structure of classical and quantum water models with the same ion–water interactions. Additionally, modeling an ion as a hard spherical solute with a point charge allows us to disentangle the response to a charge from any added complications due to van der Waals interactions. We also find that the qualitative features found for these simple ions hold for more realistic ion models, as detailed below.

We consider three general classes of water models. The most accurate model used here is the quantum-mechanics-based description of water provided by density functional theory (DFT) at the level of the revised Perdew–Burke–Ernzerhof (revPBE) generalized gradient approximation,<sup>39,40</sup> with the added dispersion correction of Grimme.<sup>41–43</sup> This model has been shown to provide a quantitatively accurate description of many properties of liquid water, including changes in the hydrogen bond network near hard sphere solutes of various sizes, which is crucial to this work.

The next two classes of models are both empirical point charge models but differ in their representation of classical lone pair electrons. This plays a key role in determining the response of the hydrogen bond network to asymmetric perturbations and strong local perturbations. In the first, the extended simple point charge (SPC/E) model of water,<sup>29</sup> the lone pair electrons are accounted for with a single charge located on the central oxygen site, effectively delocalizing them. We find that SPC/E is representative of an entire class of water models with delocalized lone pairs, and similar models like TIP4P<sup>44</sup> and its variants yield qualitatively the same results. The last type of model studied is a classical model with explicit (or localized) lone pair sites, the TIP5P model of water.<sup>30</sup> Models in this class are more symmetric in their treatment of lone pair and hydrogen sites, since both are treated as point charges tetrahedrally displaced from the oxygen core. This apparently subtle difference in the representation of lone pair electrons has already been shown to lead to significant differences in the hydration structure of uncharged solutes,<sup>22</sup> and it seems very plausible that this qualitative difference could also play a key role in the asymmetric response to the ion charge.

Average measures of the solvation structure around the model ion, like the nonuniform densities of water around the solute,<sup>22</sup> show little difference between models. Despite this model insensitivity of the angularly averaged density response, fluctuations and the orientational structure of hydration water are strongly dependent on the description of the electronic structure of water. Such orientational structure is important in determining the free energetics of charging an uncharged (ionic) core, in addition to being relevant to spectroscopic probes of solvation<sup>45–47</sup> and interface structure.<sup>7,48–51</sup> Here, we quantify the orientational preferences of hydration water by monitoring two angles with respect to the vector connecting the water oxygen and the model ion: the angle formed by the dipole moment of water,  $\theta$ , and the angle formed by the projection of this vector onto the local  $xy$  plane,  $\varphi$ . This local coordinate system uniquely defines the orientation of a water molecule.<sup>22,52</sup>

All models yield qualitatively the same hydration structure around anions; O–H bonds point directly toward the negative ion forming hydrogen bonds. In contrast, distinct differences in the hydration structure between models are found for both the uncharged and cationic spheres.

In the case of cationic hydration, water molecules tend to orient their dipoles directly away from the solute. This is illustrated by the description of water provided by van der

Waals corrected revPBE DFT simulations that provide an accurate first-principles description of the H-bond structure in water. Note that, although there is a significant size dependence to ion hydration, similar conclusions can be drawn regarding the model dependence of the absolute orientation of water around neutral and charged hard spheres for larger cavities, as is discussed further in the [Supporting Information](#). The SPC/E model tends to point its dipole moment away from the anion, with orientations obtained by rotating about this dipole vector having high probability. In contrast, TIP5P water tends to point one of its lone pair sites directly toward the cation, in a manner completely analogous to pointing an O–H bond toward an anion, with rotations about the dipole moment vector hindered due to the inflexibility of the H-bond network. The revPBE model of water yields structures between the SPC/E and TIP5P limits, albeit in somewhat better agreement with SPC/E. Thus, delocalized classical models like SPC/E may capture the hydration structure around cationic solutes, while those with explicit lone pair sites cannot.

We also find a similar model dependence around uncharged hard sphere solutes, as detailed previously<sup>22</sup> and shown in [Figure 1](#). However, around apolar solutes, the TIP5P model of

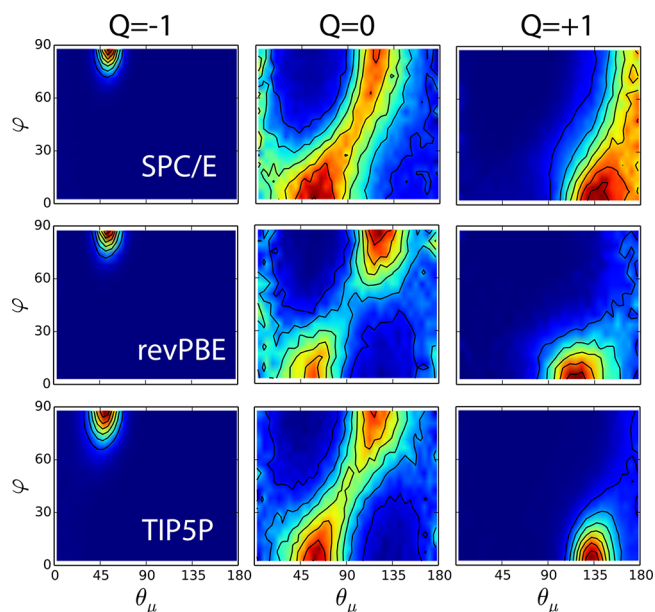


**Figure 1.** Matrix of probability distributions of water orientations in the first hydration shell of charged and uncharged hard spherical solutes with a radius of  $R_{\text{HS}} = 2.6$  Å. The top row is for SPC/E water, the middle row is for the revPBE-D3 DFT description of water, and the bottom row is for the TIP5P model of water. The left, center, and right columns correspond to hard sphere charges of  $Q = -1$ , 0, and  $+1$ , respectively. Variations in the solid angle have been removed.

water is more consistent with DFT results, while SPC/E water leads to a hydration shell that is too asymmetric with respect to the tetrahedrality of water. These findings indicate that, around an uncharged, apolar solute, water is best represented with a TIP5P-like model, while water more closely resembles SPC/E water around cations; all models yield the same qualitative hydration structure around anions. This clearly indicates that these two empirical, point charge models of water, which are representative of two general classes of fixed point charge models—those with and without explicit lone pairs—cannot simultaneously describe the hydration of apolar and cationic solutes.

## LONE-PAIR-DEPENDENT RESPONSE TO CHARGING

In addition to the significant model dependencies observed for neutral and positively charged model ions, the representation of lone pairs impacts the entire process of charging the hard sphere, which is relevant for determining charging free energies. Thus, we also investigated the changes in orientational structure that occur upon slowly charging a hard sphere of radius 2.6 Å from  $Q = 0$  to  $Q = \pm 1$  in increments of  $\Delta Q = \pm 0.1$ . The structural changes are clearly visualized through the one-dimensional distributions  $P(\theta_\mu)$  and  $P(\varphi)$ . Charging in the negative directions is similar for all models, as shown in Figure S2. In contrast, significant differences are observed when charging to  $Q = +1$ , as shown in Figure 2 and expected from the results discussed above.

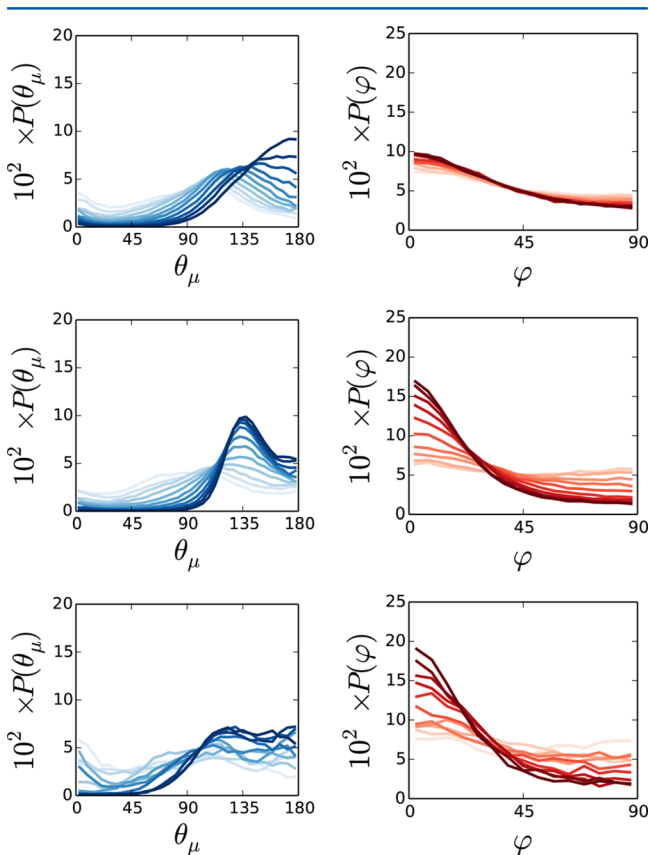


**Figure 2.** Probability distributions of water orientations (left)  $P(\theta_\mu)$  and (right)  $P(\varphi)$  for the (top) SPC/E, (middle) TIPSP, and (bottom) revPBE-D3 water models. Darker lines indicate larger  $Q$ , and are plotted from  $Q = 0$  to  $Q = +1$  in increments of  $\Delta Q = 0.1$ . Variations in the solid angle have been removed.

In the case of SPC/E water, with delocalized electron density around the oxygen site,  $P(\varphi)$  does not significantly change upon moving from a hard sphere to a cation. The dominant structural change is in the orientation of the water dipoles, with  $P(\theta_\mu)$  shifting from a bimodal distribution at  $Q = 0$  to a unimodal distribution at  $Q = 1$  with a peak growing in at  $\theta_\mu = 180^\circ$ . This behavior is quite different from what is observed in the case of the TIPSP water model with explicit, localized lone pair sites. In this case, significant changes in  $P(\varphi)$  and  $P(\theta_\mu)$  occur upon charging as the water molecules reorient to point a lone pair site directly toward the cation. This is evidenced by

the peak forming near  $\theta_\mu = 135^\circ$  in  $P(\theta_\mu)$  as the solute is charged.

The DFT description of liquid water displays behavior between the two classical limits.  $P(\varphi)$  is found to be very similar to that of TIPSP water. However,  $P(\theta_\mu)$  is significantly different from both the SPC/E and TIPSP limits. Probability increases at both  $\theta_\mu = 135^\circ$  and  $\theta_\mu = 180^\circ$  as the solute is charged, with significantly more probability at lower values of  $\theta_\mu$  than observed in the classical models. This finding highlights the flexibility of the H-bond network and electronic density in quantum mechanical descriptions of liquid water that are not captured in classical models with rigid charge distributions. The DFT-based model can act (structurally) as if it has localized lone pairs and delocalized charge density in different contexts, spanning TIPSP- and SPC/E-like structures.

## LOCAL RESPONSE IS DUE TO SHORT-RANGED FORCES

The local hydration structure around these solutes is dictated by strong, short-ranged interactions. We illustrate this point by performing simulations of the classical models with truncated electrostatic interactions using the formalism of local molecular field theory.<sup>53–56</sup> Namely, we separate the Coulomb potential according to

$$v(r) = \frac{1}{r} = \frac{\text{erfc}(r/\sigma)}{r} + \frac{\text{erf}(r/\sigma)}{r} \equiv v_0(r) + v_1(r) \quad (2)$$

where the smoothing length  $\sigma$  at which the potential is separated is chosen on the order of the nearest-neighbor distance in water, here  $\sigma = 4.5$  Å. The short-ranged potential  $v_0(r)$  varies rapidly over  $\sigma$ , while the long-ranged  $v_1(r)$  varies slowly over all distances. Previous work has emphasized that replacing the full Coulomb interaction with only  $v_0(r)$ , leading to so-called *Gaussian-truncated* (GT) models, gives a good representation of the short-ranged interactions and local structural features in many molecular systems.<sup>54–57</sup>

We performed simulations with GT variants of the classical SPC/E and TIPSP models and of the ions to illustrate that short-ranged interactions determine the orientational structure of water in the hydration shell of the model ionic solutes discussed here. The probability distributions characterizing the orientational structure of the short-ranged GT systems, shown in Figure S3, are nearly identical to those obtained for the full systems, shown in Figure 1. The truncated electrostatic models explicitly illustrate that the structure of the first hydration shell around ionic solutes is determined exclusively by short-ranged interactions arising from excluded volume and local electrostatic interactions, which result in an interplay of water–water and ion–water hydrogen bonding. This finding is in accord with a wealth of experimental data suggesting that ionic solutes perturb mainly the first hydration shell of water.<sup>7,58–61</sup>

## LONG-RANGED ELECTROSTATIC RESPONSE IS MODEL INDEPENDENT AND FOLLOWS DIELECTRIC CONTINUUM THEORY

Significant differences among the water models are observed when short-ranged interactions dominate the hydration of ionic solutes, arising from an interplay between excluded volumes and local hydrogen bonds. However, long-ranged interactions leading to macroscopic dielectric response should be model-independent and only reliant on the dielectric constant of water. Here, we illustrate this point by monitoring the response

of classical and quantum water models to the long-ranged potential  $v_1(r)$  only, in the absence of any excluded volume core. This is equivalent to inserting a Gaussian test charge distribution into solution,<sup>23</sup> the finite value of this potential at small distances removes the delta-function singularity that prohibits carrying out this procedure with an isolated point charge. The potential from this Gaussian charge is chosen to vary slowly over molecular length scales ( $\sigma = 3.2$  Å), and we expect the solvent to respond linearly to this perturbation. Moreover, as described recently,<sup>23</sup> the response of the solvent charge density  $\rho^q(r)$  to a slowly varying test charge distribution  $\rho^Q(r)$  is linear, with the dielectric solvent locally screening or canceling all but a fraction  $1/\epsilon$  of the applied charge distribution

$$\rho^q(r) = -\left(1 - \frac{1}{\epsilon}\right)\rho^Q(r) \quad (3)$$

where  $\epsilon$  is the dielectric constant of water. Thus, classical and quantum descriptions of water will yield a similar response to  $\rho^Q(r)$  if DFT accurately describes the dielectric constant of water.

We monitor the structural response of water through the charge density,  $\rho^q(\mathbf{r})$ , and the Gaussian-smoothed charge density,  $\rho^{q\sigma}(\mathbf{r})$ , defined as the convolution of  $\rho^q(\mathbf{r})$  with a Gaussian distribution of width  $\sigma$ . The smoothed charge density  $\rho^{q\sigma}(\mathbf{r})$  has been shown to provide a good characterization of the underlying long-ranged response of molecular systems to electrostatic perturbations.<sup>23,53,62</sup> The charge densities obtained in the presence of an anionic Gaussian test charge are compared in Figure 3. Note that the test charge, and therefore the response, is not rigorously a Gaussian density because Ewald summation leads to appreciable finite size effects; see the Supporting Information for further discussion of these and other subtleties.

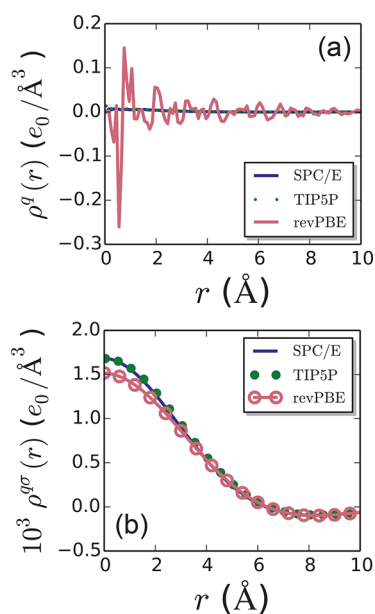


**Figure 3.** (a) Charge densities,  $\rho^q(r)$ , and (b) Gaussian-smoothed charge densities,  $\rho^{q\sigma}(r)$ , in response to a Gaussian test charge with a width of 3.2 Å and  $Q = -1$ . Gaussian smoothed charge densities were obtained by convoluting  $\rho^q(r)$  with a Gaussian distribution of width  $\sigma = 3.2$  Å.

Significant differences in  $\rho^q(r)$  are observed due to vastly different magnitudes of charge fluctuations in the quantum and classical models. However, the long-ranged response relevant to dielectric response and captured by  $\rho^{q\sigma}(r)$  is model independent; the small differences at small  $r$  arise from simulation noise due to limited sampling in the quantum case. This level of agreement between models demonstrates that both empirical point charge and quantum DFT descriptions provide an equivalent and highly accurate description of the dielectric response of liquid water. In the context of reduced models of ion hydration, our findings illustrate that modifications incorporating atomistic details are only necessary for local hydration structure, and long-ranged effects can still be captured with simple DCT concepts relying on the dielectric constant. The model independence of long-ranged effects is also expected to be true for ion association, where the potential of mean force between ions at large distances can be predicted with DCT, while the short-ranged behavior is dominated by local interactions and is highly model dependent.<sup>63–66</sup>

### ■ MORE COMPLEX DESCRIPTIONS OF IONIC SOLUTES AMPLIFY DEFICIENCIES OF EMPIRICAL MODELS OF HYDRATION

Real ions are much more complex than the simple hard sphere plus point charge models studied in this work. However, our qualitative findings regarding solvation structure are unchanged by using more physical models of ion–water interactions. For quantum-mechanics-based models of water, this corresponds to a similar *ab initio* treatment of ions using DFT. Such a treatment includes complex features like electronic polarizability of both the ion and water, in addition to van der Waals interactions, albeit by using a simplistic correction in this case; more complex functionals explicitly incorporating exact exchange and nonlocal interactions are not expected to change our qualitative findings. In the classical description of empirical models, an ion is typically modeled as a LJ sphere with a point charge at its center, lacking polarizability in many cases, although such models have been developed.<sup>67,68</sup>

We illustrate our findings using  $\text{Na}^+$  and  $\text{Cl}^-$  ions, chosen because they are colloquially considered to be a case where classical descriptions are nearly as good as more complex quantum models. Orientational distributions are shown in Figure 4 for both first-principles and empirical descriptions of ionic hydration. The hydration structure around chloride is similar for all systems, in agreement with what was found for anionic hard spheres. However, qualitative differences among all models are observed in the case of sodium hydration, with the DFT model adopting an orientation somewhat in between the extremes of SPC/E and TIP5P. In fact, the individual orientational probability distributions obtained for revPBE water around the five  $\text{Na}^+$  ions that are averaged to obtain the data in Figure 4, shown in the Supporting Information, clearly indicate that the DFT model adopts structures consistent with the SPC/E-like and TIP5P-like limits, as well as structures in between these limits. This further strengthens the earlier conclusion that empirical fixed-charge models cannot describe the hydration of ionic and nonpolar species simultaneously. Moreover, previous work has shown that more complex polyatomic ions can adopt electronic structures that are completely different from the simple methods used to construct standard empirical models, implying that such classical potentials are unable to describe their hydration structure.<sup>69</sup>

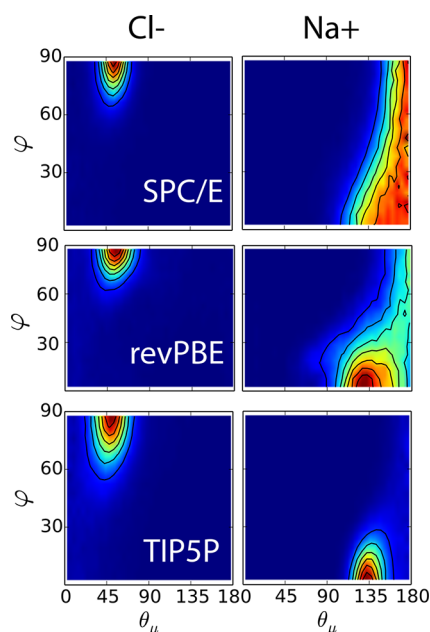


**Figure 4.** Probability distributions of the orientational structure of water molecules in the first hydration shell of (left column)  $\text{Cl}^-$  and (right column)  $\text{Na}^+$ . Data are shown for (top row) SPC/E, (middle row) revPBE-D3, and (bottom row) TIP5P descriptions of water. Also note that the classical ions are treated as nonpolarizable, empirical potentials in the SPC/E and TIP5P systems, such that  $\text{Cl}^-$  and  $\text{Na}^+$  are charged Lennard-Jones spheres. In contrast, the ions are treated within DFT in the *ab initio* systems. Variations in the solid angle have been removed.

The accuracy of our *ab initio* models, to which we compare the empirical SPC/E and TIP5P potentials, is supported by numerous experimental results.<sup>58</sup> A classic neutron diffraction study by Soper et al. suggested that water molecules tend to orient their O–H bonds toward anions in a manner completely analogous to our findings.<sup>70</sup> In the same study, evidence for hydration waters to orient their dipoles away from cations was also found.<sup>70</sup> More recently, a combination of femtosecond time-resolved infrared and terahertz dielectric relaxation spectroscopies<sup>47</sup> revealed that the dynamics of water molecules in ionic hydration shells are consistent with the orientational preferences described here. This evidence suggests that the microscopic description of water provided by the DFT-based techniques used here is reasonably accurate, although deficiencies have been noted for the hydration of some ions.<sup>71</sup>

#### ■ IMPLICATIONS FOR MODELS OF ION HYDRATION

Continuum models of dielectric phenomena, like the solvation of ionic and dipolar solutes, by definition neglect atomic features of the solvent. In this work, we have demonstrated that such atomistic details have a profound impact on the hydration structure and consequently the macroscopic thermodynamics of solute hydration. The hydration structure impacts the charging free energy of a hard sphere through the relevant electrostatic potential difference between the bulk and inside the core,  $\Delta\phi_C$ , which depends sensitively on the orientation of water molecules at the solute surface and their charge distribution. The corresponding charging free energy is

$$\Delta G_Q = Q \int_0^1 d\lambda \langle \Delta\phi_C \rangle_\lambda \quad (4)$$

where  $\lambda$  is a coupling parameter used to change the charge from zero to  $Q$  and  $\langle \dots \rangle_\lambda$  indicates an ensemble average when sampling is performed in the presence of an ionic charge equal to  $\lambda Q$ . Thus, for a model to have even qualitative success, it must include some representation of the atomistic details of the local response of water to the nanoscale broken symmetries presented by a solute.

The deficiencies in the classical models in estimating ion hydration thermodynamics can be clearly observed by comparing the extent of the cation–anion asymmetry,  $\Delta\Delta G = \Delta G_- - \Delta G_+$ , for a hard sphere ion with a core size of 2.6 Å, where  $\Delta G$  refers to the real single ion solvation free energies, which reference the zero of the electrostatic potential to the vacuum phase. For the revPBE model,<sup>34</sup> the asymmetry is  $\beta\Delta\Delta G^{\text{revPBE}} = -88$ , while SPC/E and TIP5P yield  $\beta\Delta\Delta G^{\text{SPC/E}} = -102$  and  $\beta\Delta\Delta G^{\text{TIP5P}} = -28$ ;  $\Delta\Delta G$  as a function of ionic charge for the classical models is shown in the Supporting Information. The TIP5P asymmetry is significantly smaller than SPC/E and revPBE, in accord with the more symmetric hydration structures produced by this model. SPC/E lies at the other extreme and has a large asymmetry due to the significantly different hydration structures of cations and anions in this model, further highlighting the effects of structure on thermodynamics. We also note that, when both the ion and water are modeled within the density functional theory framework, the asymmetry produced by the revPBE is largely canceled by a large exchange contribution to the solvation free energy.<sup>72</sup>

The thermodynamically relevant portion of the electrostatic potential inside a solute core is a molecular-level detail that must be incorporated into theoretical descriptions of ionic hydration. There are two components of this potential, one arising from boundaries, like a liquid–vapor interface far from the solute or the excluded volume core of the hydrated ion, and a component due to the structural response to the ionic charging. The former arises from structural perturbations that exist even in the absence of ionic charge, and its contribution to the charging free energy does not require knowledge of the charging process. The latter contribution is more complex, and we have shown that rigid classical models cannot describe the structural response to an ion over the entire charging process, as provided by DFT calculations. Recent DFT calculations<sup>34</sup> illustrate that the charging process can also have significant nonlinearities that will additionally complicate any theoretical treatment.

Our findings illustrate the importance of the flexibility of the underlying charge distribution of water in determining hydration structures and thermodynamics, and previous work has highlighted its impact in understanding the hydrogen bond dynamics of water.<sup>28</sup> Despite the quantitative inaccuracies associated with using a GGA-level functional, the DFT-based model used here highlights that quantum water models can adopt a range of structures spanning the TIP5P-like and SPC/E-like limits, and that the charge distribution of water may not have a fixed form, even qualitatively. Thus, most polarizable models, which typically also assume a fixed underlying charge distribution of water on which to place Drude oscillators or similar fluctuating electrostatic multipoles, may not be able to capture this inherent flexibility of the electronic structure of water. However, for many properties of aqueous solutions, empirical point charge models and their extensions will remain at the center of many investigations, and this study aids in understanding the strengths and limitations of such models.

It would be of interest to determine if intermolecular potentials obtained by different routes, such as neural network or other machine-learning-based approaches,<sup>73,74</sup> can capture the inherent flexibility of quantum-mechanics-based models, with and without the explicit inclusion of configurations that span the range of configurations obtained with localized and delocalized lone electron pairs. In these approaches, one should train with higher levels of theory than that used here, including new accurate density functionals,<sup>75,76</sup> coupled-cluster theories,<sup>77–79</sup> and random phase approximations.<sup>80</sup> The subtleties in ion hydration structures involve a delicate interplay between direct ion–water interactions and the response of the hydrogen bond network to the constraints imposed by solvating the ion. Thus, any such training will need to incorporate a description of hydration structure, including the charging process in the condensed phase. Although GGA-level DFT functionals are known to be deficient in capturing the energetics of configurations as compared to coupled-cluster theories,<sup>75</sup> this work suggests that attention to the fluctuations in the energy of ion–water interactions could be an important aspect in capturing complex collective phenomena. Indeed, the average ion–water energetics are important to capture solvation free energies. However, if efficient quantum-mechanics-based models at the GGA level provide the correct structures and fluctuations in the energetics, simple corrections based on efficient resampling of representative clusters at correlated wave function levels of theory can be straightforwardly implemented to correct solvation free energies.<sup>72</sup>

## ■ ASSOCIATED CONTENT

### Supporting Information

The Supporting Information is available free of charge on the ACS Publications website at DOI: 10.1021/acs.jpcc.7b10722.

A discussion of the relation between the Born radius and the nonuniform dielectric constant, results for the 4 Å hard sphere solutes, analogues of Figure 2 for charging in the anionic direction, a characterization of orientational solvation structure in truncated models, discussions of the subtleties associated with Gaussian charge solvation, plot of the asymmetry in the ion hydration free energy for the SPC/E and TIP5P models, and orientational structure of revPBE-D3 water around five independent Na<sup>+</sup> ions (PDF)

## ■ AUTHOR INFORMATION

### Corresponding Authors

\*E-mail: rremensing@temple.edu.

\*E-mail: chris.mundy@pnnl.gov.

\*E-mail: jdw@umd.edu.

### ORCID

Timothy T. Duignan: 0000-0003-3772-8057

Christopher J. Mundy: 0000-0003-1378-5241

John D. Weeks: 0000-0003-3764-3715

### Notes

The authors declare no competing financial interest.

## ■ ACKNOWLEDGMENTS

T.T.D., G.K.S., and C.J.M. were supported by the U.S. Department of Energy, Office of Science, Office of Basic Energy Sciences, Division of Chemical Sciences, Geosciences, and Biosciences. M.D.B. was supported by the MS<sup>3</sup> (Materials

Synthesis and Simulation Across Scales) Initiative, a Laboratory Directed Research and Development Program at Pacific Northwest National Laboratory (PNNL). PNNL is a multi-program national laboratory operated by Battelle for the U.S. Department of Energy. J.D.W. and R.C.R. acknowledge funding from National Science Foundation Grants CHE0848574 and CHE1300993. This research used resources of the National Energy Research Scientific Computing Center, a DOE Office of Science User Facility supported by the Office of Science of the U.S. DOE under Contract No. DE-AC02-05CH11231.

## ■ REFERENCES

- (1) Collins, K. D. Why Continuum Electrostatics Theories Cannot Explain Biological Structure, Polyelectrolytes or Ionic Strength Effects in Ion-Protein Interactions. *Biophys. Chem.* **2012**, *167*, 43–59.
- (2) Moreira, L. A.; Boström, M.; Ninham, B. W.; Biscaia, E. C.; Tavares, F. W. Hofmeister Effects: Why Protein Charge, PH Titration and Protein Precipitation Depend on the Choice of Background Salt Solution. *Colloids Surf, A* **2006**, *282–283*, 457–463.
- (3) England, J. L.; Haran, G. Role of Solvation Effects in Protein Denaturation: From Thermodynamics to Single Molecules and Back. *Annu. Rev. Phys. Chem.* **2011**, *62*, 257–77.
- (4) Canchi, D. R.; García, A. E. Cosolvent Effects on Protein Stability. *Annu. Rev. Phys. Chem.* **2013**, *64*, 273–93.
- (5) Chang, T.-M.; Dang, L. X. Recent Advances in Molecular Simulations of Ion Solvation at Liquid Interfaces. *Chem. Rev.* **2006**, *106*, 1305–1322.
- (6) Knipping, E. M.; Lakin, M. J.; Foster, K. L.; Jungwirth, P.; Tobias, D. J.; Gerber, R. B.; Dabdub, D.; Finlayson-Pitts, B. J. Experiments and Simulations of Ion-Enhanced Interfacial Chemistry on Aqueous NaCl Aerosols. *Science* **2000**, *288*, 301–306.
- (7) Geissler, P. L. Water Interfaces, Solvation, and Spectroscopy. *Annu. Rev. Phys. Chem.* **2013**, *64*, 317–37.
- (8) Tobias, D. J.; Stern, A. C.; Baer, M. D.; Levin, Y.; Mundy, C. J. Simulation and Theory of Ions at Atmospherically Relevant Aqueous Liquid-Air Interfaces. *Annu. Rev. Phys. Chem.* **2013**, *64*, 339–59.
- (9) Netz, R. R.; Horinek, D. Progress in Modeling of Ion Effects at the Vapor/water Interface. *Annu. Rev. Phys. Chem.* **2012**, *63*, 401–18.
- (10) Born, M. Volumes and Hydration Warmth of Ions. *Eur. Phys. J. A* **1920**, *1*, 45–48.
- (11) Rashin, A. A.; Honig, B. Reevaluation of the Born Model of Ion Hydration. *J. Phys. Chem.* **1985**, *89*, 5588–5593.
- (12) Jayaram, B.; Fine, R.; Sharp, K.; Honig, B. Free Energy Calculations of Ion Hydration: An Analysis of the Born Model in Terms of Microscopic Simulations. *J. Phys. Chem.* **1989**, *93*, 4320–4327.
- (13) Rajamani, S.; Ghosh, T.; Garde, S. Size Dependent Ion Hydration, Its Asymmetry, and Convergence to Macroscopic Behavior. *J. Chem. Phys.* **2004**, *120*, 4457–4466.
- (14) Bardhan, J. P.; Jungwirth, P.; Makowski, L. Affine-Response Model of Molecular Solvation of Ions: Accurate Predictions of Asymmetric Charging Free Energies. *J. Chem. Phys.* **2012**, *137*, 124101.
- (15) Ashbaugh, H. S. Convergence of Molecular and Macroscopic Continuum Descriptions of Ion Hydration. *J. Phys. Chem. B* **2000**, *104*, 7235–7238.
- (16) Harder, E.; Roux, B. On the Origin of the Electrostatic Potential Difference at a Liquid-Vacuum Interface. *J. Chem. Phys.* **2008**, *129*, 234706.
- (17) Hunenberger, P.; Reif, M. *Single-Ion Solvation: Experimental and Theoretical Approaches to Elusive Thermodynamic Properties*; RCS: Cambridge, 2011; Vol. 3.
- (18) Baer, M. D.; Stern, A. C.; Levin, Y.; Tobias, D. J.; Mundy, C. J. Electrochemical Surface Potential Due to Classical Point Charge Models Drives Anion Adsorption to the Air-Water Interface. *J. Phys. Chem. Lett.* **2012**, *3*, 1565–1570.
- (19) Beck, T. L. The Influence of Water Interfacial Potentials on Ion Hydration in Bulk Water and Near Interfaces. *Chem. Phys. Lett.* **2013**, *561–562*, 1–13.

- (20) Shi, Y.; Beck, T. L. Length Scales and Interfacial Potentials in Ion Hydration. *J. Chem. Phys.* **2013**, *139*, 044504.
- (21) Horváth, L.; Beu, T.; Manghi, M.; Palmeri, J. The Vapor-Liquid Interface Potential of (multi)polar Fluids and Its Influence on Ion Solvation. *J. Chem. Phys.* **2013**, *138*, 154702.
- (22) Remsing, R. C.; Baer, M. D.; Schenter, G. K.; Mundy, C. J.; Weeks, J. D. The Role of Broken Symmetry in Solvation of a Spherical Cavity in Classical and Quantum Water Models. *J. Phys. Chem. Lett.* **2014**, *5*, 2767–2774.
- (23) Remsing, R. C.; Weeks, J. D. Role of Local Response in Ion Solvation: Born Theory and Beyond. *J. Phys. Chem. B* **2016**, *120*, 6238–6249.
- (24) Duignan, T. T.; Parsons, D. F.; Ninham, B. W. a Continuum Solvent Model of the Multipolar Dispersion Solvation Energy. *J. Phys. Chem. B* **2013**, *117*, 9412–9420.
- (25) Duignan, T. T.; Parsons, D. F.; Ninham, B. W. a Continuum Model of Solvation Energies Including Electrostatic, Dispersion, and Cavity Contributions. *J. Phys. Chem. B* **2013**, *117*, 9421–9429.
- (26) Duignan, T. T.; Parsons, D. F.; Ninham, B. W. Collins's Rule, Hofmeister Effects and Ionic Dispersion Interactions. *Chem. Phys. Lett.* **2014**, *608*, 55–59.
- (27) Pollard, T. P.; Beck, T. L. Toward a Quantitative Theory of Hofmeister Effects: From Quantum Effects to Thermodynamics. *Curr. Opin. Colloid Interface Sci.* **2016**, *23*, 110–118.
- (28) Agmon, N. Liquid Water: From Symmetry Distortions to Diffusive Motion. *Acc. Chem. Res.* **2012**, *45*, 63–73.
- (29) Berendsen, H. J. C.; Grigera, J. R.; Straatsma, T. P. The Missing Term in Effective Pair Potentials. *J. Phys. Chem.* **1987**, *91*, 6269–6271.
- (30) Mahoney, M.; Jorgensen, W. A Five-Site Model for Liquid Water and the Reproduction of the Density Anomaly by Rigid, Nonpolarizable Potential Functions. *J. Chem. Phys.* **2000**, *112*, 8910–8922.
- (31) Smith, W.; Yong, C.; Rodger, P. DL\_POLY: Application to Molecular Simulation. *Mol. Simul.* **2002**, *28*, 385–471.
- (32) Berendsen, H. J. C.; Postma, J. P. M.; van Gunsteren, W. F.; DiNiola, A.; Haak, J. R. Molecular Dynamics with Coupling to an External Bath. *J. Chem. Phys.* **1984**, *81*, 3684–3690.
- (33) Allen, M. P.; Tildesley, D. J. *Computer Simulation of Liquids*; Oxford: New York, 1987.
- (34) Duignan, T. T.; Baer, M. D.; Schenter, G. K.; Mundy, C. J. Electrostatic Solvation Free Energies of Charged Hard Spheres Using Molecular Dynamics with Density Functional Theory Interactions. *J. Chem. Phys.* **2017**, *147*, 161716.
- (35) Horinek, D.; Herz, A.; Vrbka, L.; Sedlmeier, F.; Mamatkulov, S. I.; Netz, R. R. Specific Ion Adsorption at the Air/water Interface: The Role of Hydrophobic Solvation. *Chem. Phys. Lett.* **2009**, *479*, 173–183.
- (36) VandeVondele, J.; Krack, M.; Mohamed, F.; Parrinello, M.; Chassaing, T.; Hutter, J. QUICKSTEP: Fast and Accurate Density Functional Calculations Using a Mixed Gaussian and Plane Waves Approach. *Comput. Phys. Commun.* **2005**, *167*, 103–128.
- (37) VandeVondele, J.; Hutter, J. Gaussian Basis Sets for Accurate Calculations on Molecular Systems in Gas and Condensed Phases. *J. Chem. Phys.* **2007**, *127*, 114105.
- (38) Goedecker, S.; Teter, M.; Hutter, J. Separable Dual-Space Gaussian Pseudopotentials. *Phys. Rev. B: Condens. Matter Mater. Phys.* **1996**, *54*, 1703–1710.
- (39) Perdew, J.; Burke, K.; Ernzerhof, M. Generalized Gradient Approximation Made Simple. *Phys. Rev. Lett.* **1996**, *77*, 3865–3868.
- (40) Zhang, Y.; Yang, W. Comment on “Generalized Gradient Approximation Made Simple”. *Phys. Rev. Lett.* **1998**, *80*, 890.
- (41) Grimme, S. Accurate Description of Van Der Waals Complexes by Density Functional Theory Including Empirical Corrections. *J. Comput. Chem.* **2004**, *25*, 1463–1473.
- (42) Grimme, S. Semiempirical GGA-Type Density Functional Constructed with Long-Range Dispersion Correction. *J. Comput. Chem.* **2006**, *27*, 1787–1799.
- (43) Grimme, S.; Antony, J.; Ehrlich, S.; Krieg, H. A Consistent and Accurate Ab Initio Parametrization of Density Functional Dispersion Correction (DFT-D) for the 94 Elements H-Pu. *J. Chem. Phys.* **2010**, *132*, 154104.
- (44) Jorgensen, W. L.; Chandrasekhar, J.; Madura, J. D.; Impey, R. W.; Klein, M. L. Comparison of Simple Potential Functions for Simulating Liquid Water. *J. Chem. Phys.* **1983**, *79*, 926–935.
- (45) Davis, J. G.; Gierszal, K. P.; Wang, P.; Ben-Amotz, D. Water Structural Transformation at Molecular Hydrophobic Interfaces. *Nature* **2012**, *491*, 582–5.
- (46) Scheu, R.; Rankin, B. M.; Chen, Y.; Jena, K. C.; Ben-Amotz, D.; Roke, S. Charge Asymmetry at Aqueous Hydrophobic Interfaces and Hydration Shells. *Angew. Chem., Int. Ed.* **2014**, *53*, 9560–3.
- (47) Tielrooij, K. J.; Garcia-Araez, N.; Bonn, M.; Bakker, H. J. Cooperativity in Ion Hydration. *Science* **2010**, *328*, 1006–1009.
- (48) Eissenthal, K. B. Liquid Interfaces Probed by Second-Harmonic and Sum-Frequency Spectroscopy. *Chem. Rev.* **1996**, *96*, 1343–1360.
- (49) Shen, Y. R.; Ostroverkhov, V. Sum-Frequency Vibrational Spectroscopy on Water Interfaces: Polar Orientation of Water Molecules at Interfaces. *Chem. Rev.* **2006**, *106*, 1140–1154.
- (50) Nihonyanagi, S.; Mondal, J. A.; Yamaguchi, S.; Tahara, T. Structure and Dynamics of Interfacial Water Studied by Heterodyne-Detected Vibrational Sum-Frequency Generation. *Annu. Rev. Phys. Chem.* **2013**, *64*, 579–603.
- (51) de Beer, A. G. F.; Roke, S. What Interactions Can Distort the Orientational Distribution of Interfacial Water Molecules As Probed by Second Harmonic and Sum Frequency Generation? *J. Chem. Phys.* **2016**, *145*, 044705.
- (52) Jedlovsky, P.; Predota, M.; Nezbeda, I. Hydration of Apolar Solutes of Varying Size: A Systematic Study. *Mol. Phys.* **2006**, *104*, 2465–2476.
- (53) Rodgers, J. M.; Weeks, J. D. Local Molecular Field Theory for the Treatment of Electrostatics. *J. Phys.: Condens. Matter* **2008**, *20*, 494206.
- (54) Chen, Y. G.; Weeks, J. D. Local Molecular Field Theory for Effective Attractions Between like Charged Objects in Systems with Strong Coulomb Interactions. *Proc. Natl. Acad. Sci. U. S. A.* **2006**, *103*, 7560–7565.
- (55) Remsing, R. C.; Rodgers, J. M.; Weeks, J. D. Deconstructing Classical Water Models at Interfaces and in Bulk. *J. Stat. Phys.* **2011**, *145*, 313–334.
- (56) Remsing, R. C.; Weeks, J. D. Dissecting Hydrophobic Hydration and Association. *J. Phys. Chem. B* **2013**, *117*, 15479–15491.
- (57) Rodgers, J. M.; Hu, Z.; Weeks, J. D. On the Efficient and Accurate Short-Ranged Simulations of Uniform Polar Molecular Liquids. *Mol. Phys.* **2011**, *109*, 1195–1211.
- (58) Ball, P. Water As an Active Constituent in Cell Biology. *Chem. Rev.* **2008**, *108*, 74–108.
- (59) Smith, J. D.; Saykally, R. J.; Geissler, P. L. The Effects of Dissolved Halide Anions on Hydrogen Bonding in Liquid Water. *J. Am. Chem. Soc.* **2007**, *129*, 13847–13856.
- (60) Cappa, C. D.; Smith, J. D.; Wilson, K. R.; Messer, B. M.; Gilles, M. K.; Cohen, R. C.; Saykally, R. J. Effects of Alkali Metal Halide Salts on the Hydrogen Bond Network of Liquid Water. *J. Phys. Chem. B* **2005**, *109*, 7046–7052.
- (61) Omta, A. W.; Kropman, M. F.; Woutersen, S.; Bakker, H. J. Negligible Effect of Ions on the Hydrogen-Bond Structure in Liquid Water. *Science* **2003**, *301*, 347–349.
- (62) Remsing, R. C.; Weeks, J. D. Hydrophobicity Scaling of Aqueous Interfaces by an Electrostatic Mapping. *J. Phys. Chem. B* **2015**, *119*, 9268–9277.
- (63) Hirata, F.; Levy, R. M. Ionic Association in Methanol and Related Solvents: An Extended RISM Analysis. *J. Phys. Chem.* **1987**, *91*, 4788–4795.
- (64) Bader, J. S.; Chandler, D. Computer Simulation Study of the Mean Forces Between Ferrous and Ferric Ions in Water. *J. Phys. Chem.* **1992**, *96*, 6423–6427.
- (65) Del Buono, G. S.; Figueirido, F. E.; Levy, R. M. Dielectric Response of Solvent Surrounding an Ion Pair: Ewald Potential Versus Spherical Truncation. *Chem. Phys. Lett.* **1996**, *263*, 521–529.



(66) Liu, W.; Wood, R. H.; Doren, D. J. Hydration Free Energy and Potential of Mean Force for a Model of the Sodium Chloride Ion Pair in Supercritical Water with Ab Initio Solute-Solvent Interactions. *J. Chem. Phys.* **2003**, *118*, 2837–2844.

(67) Dang, L. X.; Chang, T.-M. Molecular Dynamics Study of Water Clusters, Liquid, and Liquid-Vapor Interface of Water with Many-Body Potentials. *J. Chem. Phys.* **1997**, *106*, 8149–8159.

(68) Ponder, J. W.; Wu, C.; Ren, P.; Pande, V. S.; Chodera, J. D.; Schnieders, M. J.; Haque, I.; Mobley, D. L.; Lambrecht, D. S.; Robert, A.; DiStasio, J.; et al. Current Status of the AMOEBA Polarizable Force Field. *J. Phys. Chem. B* **2010**, *114*, 2549–2564.

(69) Baer, M. D.; Pham, V.-T.; Fulton, J. L.; Schenter, G. K.; Balasubramanian, M.; Mundy, C. J. *J. Phys. Chem. Lett.* **2011**, *2*, 2650–2654.

(70) Soper, A. K.; Neilson, G. W.; Enderby, J. E.; Howe, R. A. A Neutron Diffraction Study of Hydration Effects in Aqueous Solutions. *J. Phys. C: Solid State Phys.* **1977**, *10*, 1793–1801.

(71) Galib, M.; Baer, M. D.; Skinner, L. B.; Mundy, C. J.; Huthwelker, T.; Schenter, G. K.; Govind, N.; Fulton, J. L. Revisiting the Hydration Structure of Aqueous Na<sup>+</sup>. *J. Chem. Phys.* **2017**, *146*, 084504.

(72) Duignan, T. T.; Baer, M. D.; Schenter, G. K.; Mundy, C. J. Real Single Ion Solvation Free Energies with Quantum Mechanical Simulation. *Chem. Sci.* **2017**, *8*, 6131–6140.

(73) Medders, G. R.; Babin, V.; Paesani, F. Development of a “First-Principles” Water Potential with Flexible Monomers. III. Liquid Phase Properties. *J. Chem. Theory Comput.* **2014**, *10*, 2906–2910.

(74) Morawietz, T.; Singraber, A.; Dellago, C.; Behler, J. How Van Der Waals Interactions Determine the Unique Properties of Water. *Proc. Natl. Acad. Sci. U. S. A.* **2016**, *113*, 8368–8373.

(75) Sun, J.; Remsing, R. C.; Zhang, Y.; Sun, Z.; Ruzsinszky, A.; Peng, H.; Yang, Z.; Paul, A.; Waghmare, U.; Wu, X.; et al. Accurate First-Principles Structures and Energies of Diversely Bonded Systems from an Efficient Density Functional. *Nat. Chem.* **2016**, *8*, 831–836.

(76) Chen, M.; Ko, H.-H.; Remsing, R. C.; Andrade, M. F. C.; Santra, B.; Sun, Z.; Selloni, A.; Car, R.; Klein, M. L.; Perdew, J. P.; et al. Ab Initio Theory and Modeling of Water. *Proc. Natl. Acad. Sci. U. S. A.* **2017**, *114*, 10846–10851.

(77) Osted, A.; Kongsted, J.; Mikkelsen, K. V.; Åstrand, P.-O.; Christiansen, O. Statistically Averaged Molecular Properties of Liquid Water Calculated Using the Combined Coupled Cluster/molecular Dynamics Method. *J. Chem. Phys.* **2006**, *124*, 124503.

(78) Spura, T.; Elgabarty, H.; Kühne, T. D. “On-The-Fly” Coupled Cluster Path-Integral Molecular Dynamics: Impact of Nuclear Quantum Effects on the Protonated Water Dimer. *Phys. Chem. Chem. Phys.* **2015**, *17*, 14355–14359.

(79) McClain, J.; Sun, Q.; Chan, G. K.-L.; Berkelbach, T. C. Gaussian-Based Coupled-Cluster Theory for the Ground-State and Band Structure of Solids. *J. Chem. Theory Comput.* **2017**, *13*, 1209–1218.

(80) Del Ben, M.; Schütt, O.; Wentz, T.; Messmer, P.; Hutter, J.; Vandevondele, J. Enabling Simulation at the Fifth Rung of DFT: Large Scale RPA Calculations with Excellent Time to Solution. *Comput. Phys. Commun.* **2015**, *187*, 120–129.